Journal of Catalysis **192,** 296–306 (2000)
doi:10.1006/jcat.2000.2848, available online at http://www.idealibrary.com on IDEAL®

Platinum Aluminophosphate Oxynitride (Pt–AlPON) Catalysts for the Dehydrogenation of Isobutane to Isobutene

Miguel Angel Centeno,[1] Muriel Debois, and Paul Grange

Unité de catalyse et chimie des matériaux divisés, Université catholique de Louvain, Croix du Sud 2 boite 17, B-1348 Louvain-la-Neuve, Belgium

Received September 20, 1999; revised January 10, 2000; accepted February 4, 2000

The catalytic dehydrogenation of isobutane to isobutene over two series of platinum-supported aluminophosphate oxynitride (Pt–AlPON) catalysts, containing different amounts of nitrogen and synthesized using two different platinum precursors, was studied. The impregnation and platinum reduction processes result in a partial loss of nitrogen and a decrease in the specific surface area of the AlPON precursors. The surface and bulk structures of the catalysts are functions of the nitrogen content of the solid. At low nitrogen contents (≤6% w/w), the nitrogen is found mainly on the surface of the catalyst as an $-NH_x$ species. Above 6% w/w, nitridation of the bulk begins. The basicity of the solids increases with increasing nitrogen content. The conditions under which synthesis takes place influence the final nitrogen content and the surface structure of the catalysts. Dehydrogenation of isobutane to isobutene of the Pt–AlPON catalyst correlates with the basicity of the catalysts. The surface structure of the solids also influences the yield of isobutene.

Key Words: **platinum aluminophosphate oxynitride; isobutane dehydrogenation.**

INTRODUCTION

The production of isobutene is expected to increase in the near future. It is estimated that the demand for isobutene will increase, because it is a reactant for the synthesis of MTBE (methyl *tert*-butyl ether), used as a gasoline additive to improve the octane number and to limit the production of oxidants (1). Of the different possibilities for producing isobutene, the catalytic dehydrogenation of isobutane is of considerable importance, because it enables us to obtain isobutene from low-cost saturated feedstocks. Numerous papers have been published on the catalytic dehydrogenation of isobutane, and a number of commercial plants are now in operation. Cr-based catalysts, mainly Cr_2O_3/Al_2O_3, are the preferred commercial catalysts (2). However some problems remain to be solved, including carbon deposition on the catalyst, the high temperatures required, and the short life of the catalyst.

Platinum-supported metallosphosphate oxynitrides, such as Pt–$M(M')$PON (M = Al, Zr; M' = Ga, Cr), are useful catalysts for the dehydrogenation of isobutane to isobutene (3–5). Metallophosphate oxynitrides are obtained by activating the oxide precursor $M(M')$PO in a flow of ammonia at high temperatures. This procedure enables the partial substitution of the oxygen atoms in the network of the phosphate oxide by nitrogen atoms (6, 7). The basicity of the oxynitrides thus obtained increases with increasing nitrogen content (8–10). One of the advantages of using the oxynitrides as supports in bifunctional catalytic reactions may be that it is possible to tailor the acid–base properties of the solid by controlling the amount of nitrogen that is introduced into the framework.

We report the catalytic dehydrogenation of isobutane to isobutene over platinum-supported aluminophosphate oxynitride (Pt–AlPON) catalysts containing different amounts of nitrogen and synthesized using two different platinum precursors. We propose that the activity is correlated with the structure and the acid–base properties of the solids.

METHODS

The amorphous aluminophosphate precursor, AlPO, with a high surface area was synthesized according to the citrate method (11). Two aqueous solutions of $Al(NO_3)_3 \cdot 9H_2O$ (Merck) and $(NH_4)H_2PO_4$ (Merck), with the same molarity to obtain an Al/P ratio of 1, were stirred for 1 h at room temperature (RT). An excess of citric acid (Merck) was then added and the mixture was stirred continuously overnight. After the evaporation of water under reduced pressure, the gel obtained was dried for 10 h at 100°C in a vacuum oven (50 mbar). Finally, the solid was calcined for 16 h at 550°C.

The AlPO precursor was activated in a flow of pure NH_3 at high temperature. Adjusting the activation temperature and duration of nitridation resulted in AlPON solids with

[1] To whom correspondence should be addressed. On leave from Departamento de Química Inorgánica e Instituto de Ciencia de Materiales de Sevilla, Universidad de Sevilla-CSIC, Centro de Investigaciones Científicas Isla de la Cartuja, E-41092 Sevilla, Spain. Fax: +34 5 4460665. E-mail: centeno@cica.es.

0021-9517/00 $35.00

different O/N ratios. These samples will be referred to as AlPONx, x being the nitrogen weight percent of the solid. Pt–AlPON catalysts were prepared by impregnation using two different platinum precursors. The AlPON support, previously dehydrated for 48 h at 100°C, was added to a solution containing a sufficient amount of $Pt(acac)_2$ dissolved in 20 ml of acetone or a sufficient amount of $Pt(NH_3)_4(NO_3)_2$ dissolved in 20 ml of acetone and 5 ml of distilled water. The slurry was stirred continuously and dried at RT or after 4–5 h at RT, 1.5 h at 50°C, and 0.5–1 h at 75°C. Five milliliters of water was added when impregnation was carried out with $Pt(NH_3)_4(NO_3)_2$, because this salt is not soluble in acetone.

To obtain the metallic platinum, Pt–AlPON catalysts were treated in a flow of N_2 and the temperature was increased from RT to 500°C at 2.5°C/min; the solid was kept at this temperature for 1 h and was then reduced in a flow of pure H_2 for 2 h at 500°C.

Pt–AlPON catalysts are referred to in the text as Pt–AlPONx-y-Z, where x is the nitrogen weight percent of the AlPON support from which they were synthesized, y is the platinum precursor used in the synthesis (a = $Pt(acac)_2$, n = $Pt(NH_3)_4(NO_3)_2$), and Z is the fresh (F) or reduced (R) state of the catalyst.

The total nitrogen contents of the AlPON and Pt–AlPON solids were determined by titration with a sulfuric acid solution of the ammonia that was liberated by means of alkaline etching at 400°C with molten KOH under N_2 atmosphere according to the reaction

$$xN^{3-} + 3x\text{KOH} \rightarrow x\text{NH}_3 + 3(x/2)\text{K}_2\text{O} + 3(x/2)\text{O}^{2-}.$$

The measurement error was calculated to be lower than 10%.

The specific surface area was measured according to the single-point BET method in a Micromeritics Flowsorb II 2300 apparatus. Before analysis, the samples were degassed for 2 h at 200°C in a flow of nitrogen.

The amount of platinum was determined in an ICP-AES Philips PV8250 spectrometer.

Platinum dispersion was determined by H_2 chemisorption in a Micromeritics ASAP 2000 apparatus. Just before analysis, the sample was outgassed for 30 min at 120°C and for 2 h at 420°C. Then it was cooled to 35°C and reduced in pure H_2 (Air Liquide, 99.999%) for 15 min at 35°C and for 1 h at 450°C. Finally, it was outgassed for 2 h at 420°C; the temperature was lowered to 35°C, the temperature at which hydrogen chemisorption takes place.

H_2 uptake was used to determine the dispersion of the metal by assuming that the hydrogen/platinum stoichiometry is 1.

In situ diffuse reflectance infrared Fourier transform spectroscopy (DRIFTS) spectra were collected with a Brucker IFS88 infrared spectrometer with KBr optics and a DTGS detector. The samples were not pretreated and were placed into a commercial controlled environmental chamber (Spectra-Tech 0030-103) that was attached to a diffuse reflectance accessory (Spectra-Tech collector). The samples were heated from RT to 500°C in a flow of N_2 at 30 ml min^{-1} (Air Liquide, 99.999%), and spectra (200 scans, 4 cm^{-1} resolution) were obtained after 1 h at this temperature. An aluminum mirror was used as the background; data are presented in the absorbance mode without treatment. Commercial software (Brucker OPUS/IR 2.2) was used to calculate the area of the DRIFTS bands after the baseline was corrected with a polynomial function. The relative error of the calculated area was lower than 25%.

The X-ray photoelectron spectroscopy (XPS) analyses were performed with an SSI X-Probe (SSX-100/206) photoelectron spectrometer (Fisons), using a monochromatized Al$K\alpha$ X-ray source (1486 ± 1 eV), at a pressure around 10^{-9} Torr (1 Torr = 133.3 N m^2). A flood gun set at 6 eV and a nickel grid placed 3 mm above the sample surface were used for charge compensation. Before analysis, the samples were heated at 120°C, twice for 15 min and once for 40 min under vacuum in the pretreatment chamber, and then degassed overnight (10^{-7} Torr) before being introduced into the analysis chamber. The binding energy was calculated with respect to the C–(C, H) component of the C_{1s} adventitious carbon fixed at 284.8 eV. The spectra were decomposed according to the least-squares fitting procedure (Fisons) with a Gaussian/Lorentzian ratio of 85/15 and after subtracting a Shirley-type nonlinear baseline. The atomic ratios were calculated from the relative intensity corrected by the elemental sensitivity factors provided by the manufacturer.

Scanning electron microscopy (SEM) analyses were performed with a Philips XL 30 ESEM-FEG microscope using a back-scattered electrons detector (BSE). The pressure in the analysis chamber was 0.9 Torr and the potential difference was 20 kV.

The dehydrogenation of isobutane to isobutene was carried out in a conventional continuous flow U-shape quartz reactor at atmospheric pressure. In order to avoid intrareactor gradients, the catalyst powder was diluted with inert quartz balls (∅ = 0.2–0.8 mm). To secure total reduction of all the platinum atoms, the catalyst (0.075 g) was activated for 1 h at 500°C in a flow of H_2/He (5/95) at 116 ml min^{-1}. The first reaction temperature (430°C) was fixed and the catalytic test begun. Initial activity was determined after 2 min of reaction. Isobutane in a flow of helium (5/95, Air Liquide isobutane N35 in helium N50) at 5.8 ml min^{-1} and hydrogen in a flow of helium (5/95, Air Liquide hydrogen N40 in helium N50) at 34.8 ml min^{-1} were used as reactants. The catalysts were tested at 430, 480, 520, and 550°C. Hydrogen was added to the reactant mixture to avoid the formation of coke and deactivation of the catalyst. An isobutane-to-hydrogen ratio of 1/6 was used, because this ratio gives the best isobutene yield (12). Reactants and products were

analyzed by gas chromatography in a Packard 428 gas chromatograph equipped with an Altech column (RSL 160; 60 m long and 0.32 mm inner diameter) using a flame ionization detector (FID). Total isobutane conversion is defined as the percentage of isobutane transformed into all products. The selectivity of isobutene is defined as the percentage of the total amount of transformed isobutane which is converted into isobutene. The yield of isobutene is obtained by multiplying the selectivity (%) by the total conversion (%) divided by 100.

RESULTS

Catalysts

Table 1 shows the physical properties of the studied solids.

The specific surface area of the solid precursors without platinum decreases as the nitrogen content increases. Impregnation affects the specific surface area and the total nitrogen content of the solids, especially those synthesized from AlPON with a high surface area and low nitrogen content. For the Pt–AlPON solids that originate from AlPON17.8, these parameters are more or less constant. The specific surface area and the nitrogen content of the catalysts synthesized from AlPON4.3, however, strongly decrease. This decrease is greater in the case of the Pt–AlPON catalysts impregnated with the $Pt(NH_3)_4(NO_3)_2$/acetone/water solution due to the presence of water; water induces the hydrolysis of the solid, a reaction which was found to proceed with a loss of nitrogen and surface area (13, 14). The reduction step induces a considerable decrease in the nitrogen content of all the solids, while the specific surface area is affected only when the solids are synthesized from AlPON4.3. A loss of 94% of the surface area, far greater than that for the Pt–AlPON4.3-n-R solid, is observed on the reduced sample of Pt–AlPON4.3-a-R compared to the fresh sample of Pt–AlPON4.3-a-F. This may be due to the difficulty in controlling the temperature during the reduction step.

The dispersion of platinum in the catalysts is very low; it is moderate (29.2%) only on Pt–AlPON4.3-n-R. The SEM micrographs (Fig. 1) reveal a regular distribution of platinum particles, with an average size of 20 nm, and some agglomerates of about 1 μm. There are more agglomerates in the low-dispersion catalysts. The lower the nitrogen content of the AlPON precursor, the higher the platinum dispersion of the Pt–AlPON catalysts. On the other hand, $Pt(NH_3)_4(NO_3)_2$ catalysts show a greater dispersion of Pt than $Pt(acac)_2$ catalysts.

DRIFTS Study

Figure 2 shows *in situ* DRIFTS spectra, obtained at 500°C for the AlPO and AlPON supports and for the fresh and the reduced Pt–AlPON catalysts, arranged according to the increasing content of nitrogen in the bulk. The differences in the qualitative DRIFTS spectra of the solids arise from the different contents of nitrogen. The AlPO sample shows hydroxyl bands of moderate intensity (POH, 3670 cm^{-1}, and AlOH, 3783 cm^{-1}), an intense P=O and PO_2 absorption centered at 1348 cm^{-1}, and a characteristic structure of bands due to stretching vibrations of Al–O and P–O below 1200 cm^{-1} (15, 16). AlPON supports and Pt–AlPON catalysts have fewer intense hydroxyl bands, and –NH–(3360 cm^{-1}) and $-NH_2$ (1558 cm^{-1}) are nitrogenous species found on their surface at this temperature. Bands

TABLE 1

Physical Properties of the Studied Solids

Sample	N content (% w/w)	N loss (%)	S_{BET} ($m^2\ g^{-1}$)	S_{BET} loss (%)	Pt content (% w/w)	Pt dispersion (%)
AlPO	—	—	316	—	—	—
Pt–AlPO-a-F	—	—	211	33	0.75	—
Pt–AlPO-a-R	—	—	210	33	0.75	1.5
AlPON4.3	4.3	—	200	—	—	—
Pt–AlPON4.3-a-F	3.4	21	170	15	0.60	—
Pt–AlPON4.3-n-F	3.1	28	81	59	0.77	—
Pt–AlPON4.3-a-R	0.8	81	11	95	0.60	7.0
Pt–AlPON4.3-n-R	0.5	88	63	68	0.77	29.2
AlPON13.3	13.3	—	130	—	—	—
Pt–AlPON13.3-a-F	11.4	14	130	0	0.89	—
Pt–AlPON13.3-n-F	9.5	29	62	52	0.96	—
Pt–AlPON13.3-a-R	5.7	57	130	0	0.89	4.0
Pt–AlPON13.3-n-R	6.2	53	62	52	0.96	5.8
AlPON17.8	17.8	—	55	—	—	—
Pt–AlPON17.8-a-F	17.8	0	55	0	0.45	—
Pt–AlPON17.8-n-F	17.4	2	55	0	1.09	—
Pt–AlPON17.8-a-R	14.4	19	55	0	0.45	2.2
Pt–AlPON17.8-n-R	13.1	25	55	0	1.09	5.5

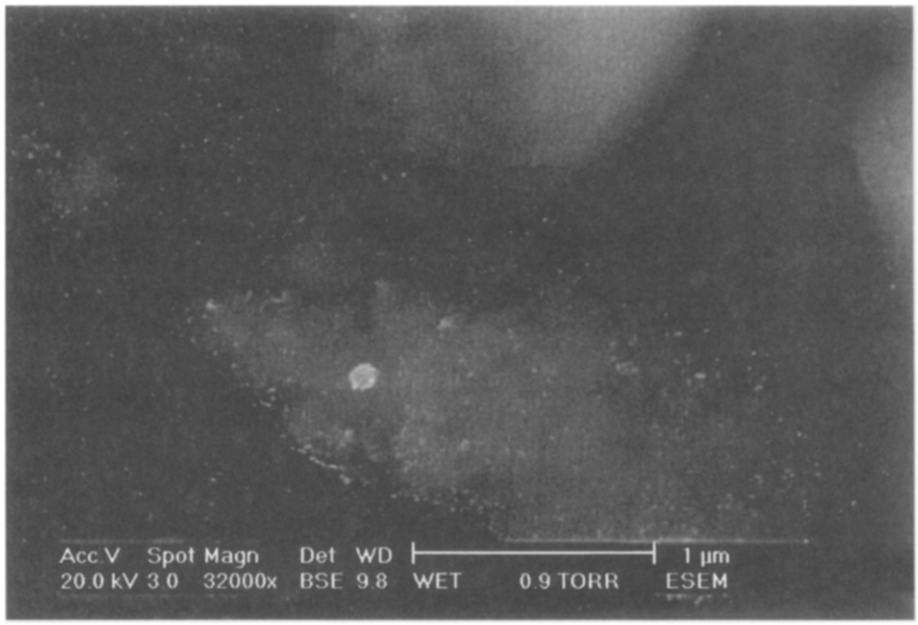

FIG. 1. SEM micrograph of Pt–AlPON4.3-n-R catalyst.

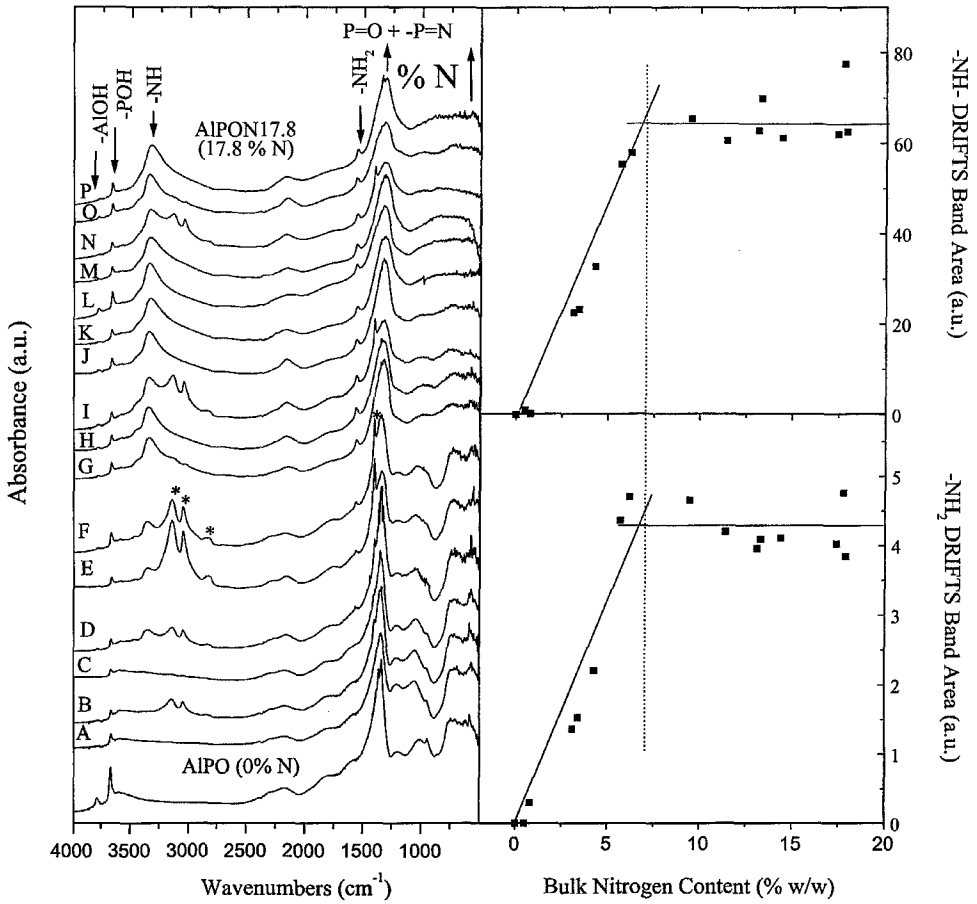

FIG. 2. (Left) *In situ* DRIFTS spectra, obtained at 500°C, of all solids studied arranged according to the increasing content of nitrogen in the bulk. (A, Pt–AlPO-a-F; B, Pt–AlPO-a-R; C, Pt–AlPON4.3-n-R; D, Pt–AlPON4.3-a-R; E, Pt–AlPON4.3-n-F; F, Pt–AlPON4.3-a-F; G, AlPON4.3; H, Pt–AlPON13.3-a-R; I, Pt–AlPON13.3-n-R; J, Pt–AlPON13.3-n-F; K, Pt–AlPON13.3-a-F; L, Pt–AlPON17.8-n-R; M, AlPON13.3; N, Pt–AlPON17.8-a-R; O, Pt–AlPON17.8-n-F; P, Pt–AlPON17.8-a-F). (Right) Quantification of the DRIFTS bands ascribed to –NH– and $-NH_2$ species as a function of the bulk nitrogen content of the solids (* DRIFTS bands of NH_4^+ ions adsorbed on the SeZn windows of the DRIFTS chamber).

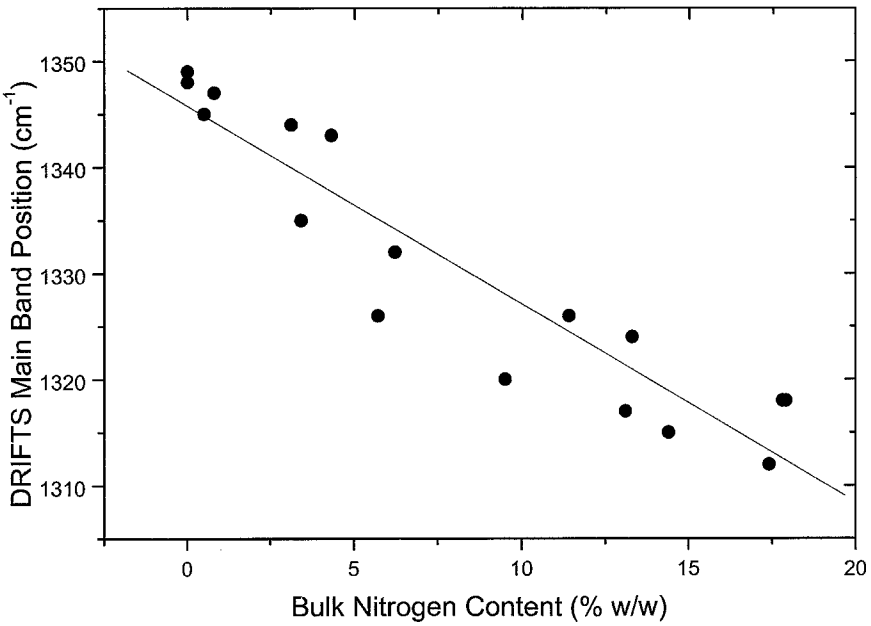

FIG. 3. Correlation between the position of the main DRIFTS band and the bulk nitrogen content of the solids.

of adsorbed NH_4^+ ions on the SeZn windows of the DRIFTS chamber are also observed at 3144, 3030, 2828, and 1400 cm^{-1} in several spectra, proving that gaseous ammonia desorbs from the surface of the catalyst during heating (13, 14). The quantification of the –NH– and $–NH_2$ DRIFTS band areas (Fig. 2) shows that the concentration of these species on the surface increases with the N content of the solid until a constant value higher than 6% is reached for the contents of N. At this level, we assume that the surface of the catalyst is saturated with these surface nitrogenous species. On the other hand, the spectra are dominated by an intense and wide absorption due to the overlapping P=O, PO_2, –P=N, and –N=P–N≡ stretching vibration bands of the solid, located in the 1320 to 1350 cm^{-1} region, its position shifting to lower wavenumbers with the nitrogen content of the solid (Fig. 3). This shift has been related to the increase in the –P=N contribution of the band (14). In fact, the wide band can be divided into three components at 1401, 1342, and 1316 cm^{-1}, assigned to P=O groups, with (1342 cm^{-1}) or without (1401 cm^{-1}) aluminum atoms in the second coordination sphere of phosphorus, and –P=N bonds (1316 cm^{-1}) (Fig. 4) (14). In good agreement with this assignment, as the content of nitrogen in the solid increases, the area of the P=O bands decreases, while that of –P=N increases (Fig. 4). Another interesting observation is that the structure below 1200 cm^{-1} is destroyed when the nitrogen content of the catalysts is above 6%. This has been observed for AlPON and AlGaPON solids and is related to the replacement of the oxygen atoms in the bulk by nitrogen (16). Thus, it is indicative of the nitridation of the solid. It is noteworthy that bulk nitridation begins at about the same content of nitrogen (≅6% w/w) as does saturation of the catalyst surface with surface nitrogenous species (–NH– and $–NH_2$). This is in good agreement with some of the proposed mechanisms that established that bulk nitridation of AlPO solids does occur once surface saturation with $–NH_2$ and –NH– groups is reached (16, 17). The removal of nitrogen through impregnation and/or reduction treatments proceeds according to a similar mechanism, affecting surface nitrogen first and then bulk nitrogen. The fact that surface nitrogenous species are detected in all solids is the result of hydrolysis of the surface of the catalysts with gaseous water, that is present under standard storage conditions, resulting in their regeneration from bulk nitrogen (13, 14).

XPS Study

Table 2 shows the binding energy values obtained for the AlPO, AlPON, and fresh and reduced Pt–AlPON series. As the nitrogen content increases the binding energy of Al, P, O, and N decreases. This shift has been assigned to a long-term interaction caused by a modified framework in which oxygen is replaced by nitrogen (17), because nitrogen is less electronegative (a better electron donor) than oxygen. The decreasing binding energy of Al and P means that these atoms behave less like electron acceptors, while the decreasing binding energy of O and N indicates that they behave more like electron donors. This behavior indicates an increase in the basicity and a decrease in the acidity of the solid with increasing nitrogen content. This has been clearly shown for AlPON solids (8). The low intensity of the platinum peaks, due to the small amount of platinum

TABLE 2

Binding Energy Values (eV) Referred to as C 1*s* (284.8 eV) for AlPO, AlPON, and Fresh and Reduced Pt–AlPON Solids as a Function of Their Nitrogen Content

Sample	N content (% w/w)	E_b (eV)						
		Al 2*s*	Al 2*p*	P 2*p*	Pt 4*f*	Pt 4*d*5	O 1*s*	N 1*s*
AlPO	—							
Pt–AlPO-a-F	—	120.2	75.3	134.7	74.8	315.1	532.3	400.7
Pt–AlPO-a-R	—	120.3	75.5	134.9	74.8	314.9	532.5	400.9
Pt–AlPON4.3-n-R	0.5	120.0	75.6	134.9	75.4	316.0	532.4	401.0
Pt–AlPON4.3-a-R	0.8	120.0	75.4	134.8	74.7	315.9	532.3	400.8
Pt–AlPON4.3-n-F	3.1	120.1	75.3	134.4	75.4	316.3	532.1	399.3
Pt–AlPON4.3-a-F	3.4	120.1	75.2	134.5	75.7	315.8	532.2	399.5
AlPON4.3	4.3	120.0	75.1	134.4	—	—	532.1	399.2
Pt–AlPON13.3-a-R	5.7	119.9	74.9	134.3	76.1	315.4	532.1	398.3
Pt–AlPON13.3-n-R	6.2	120.1	75.3	134.5	76.9	316.1	532.3	398.8
Pt–AlPON13.3-n-F	9.5	119.7	74.8	134.0	76.4	316.3	531.9	398.8
Pt–AlPON13.3-a-F	11.4	119.8	74.9	134.1	76.3	315.9	532.0	398.5
Pt–AlPON17.8-n-R	13.1	119.6	74.7	133.9	76.1	315.5	531.9	398.2
AlPON13.3	13.3	119.6	74.8	133.8	—	—	531.9	398.2
Pt–AlPON17.8-a-R	14.4	119.8	75.0	134.2	76.4	316.0	532.0	398.3
Pt–AlPON17.8-n-F	17.4	119.3	74.4	133.6	76.0	315.8	531.6	398.4
AlPON17.8	17.8	119.6	74.7	133.8	—	—	531.9	
Pt–AlPON17.8-a-F	17.8	119.5	74.7	133.6	74.7	315.7	531.7	398.2

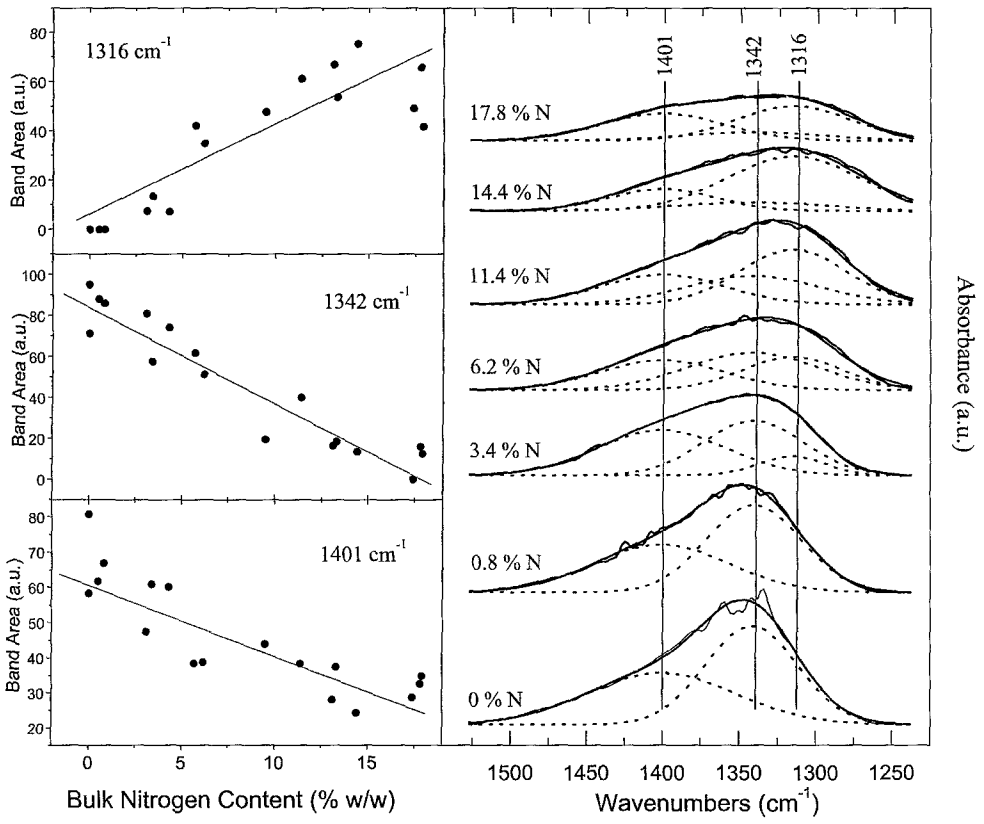

FIG. 4. (Right) Decomposition of the main DRIFTS band in the framework of the solids as a function of the total nitrogen content. (Left) Quantification of the DRIFTS bands resulting from the decomposition.

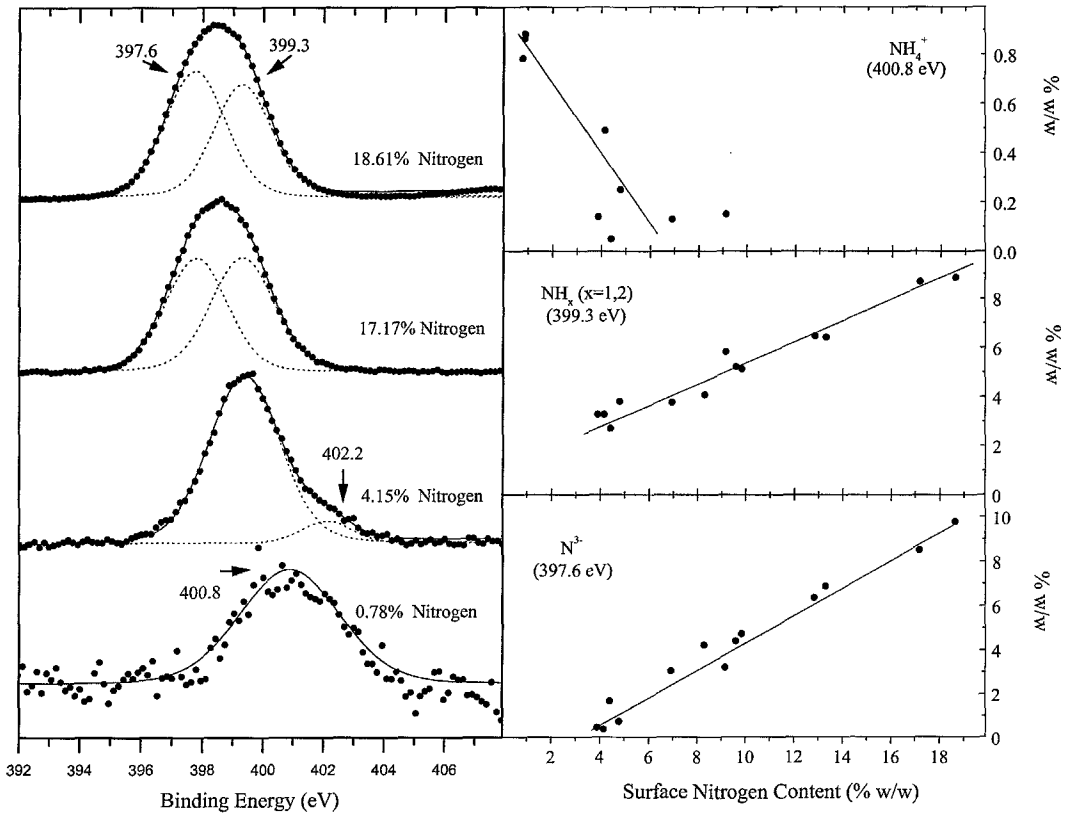

FIG. 5. (Left) N 1*s* XPS spectra of the solids as a function of the total nitrogen content of the surface. The relative intensity of each spectrum has been normalized. (Right) Evolution of the surface nitrogenous species as a function of the total surface nitrogen content.

(≈1% w/w), makes the error in the value of its binding energy very high.

Al, P, and O peaks fit a singular component quite well; however, the shape of the N 1*s* peak shows some asymmetry and changes with the nitrogen content, making a decomposition treatment necessary (Fig. 5). At low nitrogen contents (<1% w/w), only one peak, at about 400.8 eV, is detected. From ≅3 to ≅4 nitrogen weight percent, this peak shifts to 402.2 eV and a second component emerges at about 399.3 eV. At higher nitrogen contents, a third component appears at about 397.6 eV, and the component at 402.2 eV disappears. The evolution of the atomic percentages for the three N 1*s* components, as a function of the XPS total nitrogen content, is also shown in Fig. 5. The assignment of these three components is not evident since >N–, =N–, –NH–, $-NH_2$, and adsorbed NH_3 and NH_4^+ species have been found on the surface of AlPON and other oxynitride systems, all of which give close N 1*s* binding energies (17–23). Fripiat *et al.* (23) observed that ZrPON samples have a similar number of N 1*s* components at similar positions and which evolved in a similar manner. After a comprehensive study of the literature, comparing it with their own results, they assigned the N 1*s* peaks as follows: 397.6 eV to structural nitrogen (>N– or =N–), 399.3 eV to NH_x ($x = 1, 2$), and 400.8 eV to adsorbed nitrogenous species (NH_3 and/or NH_4^+). The peak that we observed at 402.2 eV at low nitrogen contents can also be assigned to adsorbed species (24). Adsorbed ammonia species are found on the surface of all the AlPON catalysts at room temperature (13, 14) and, in most cases, disappear after pretreatment (120°C under 10^{-6} Torr vacuum). Only in solids with very low contents of nitrogen, which are more acidic (8–10), are these species still found on the surface after pretreatment; they are strongly attached to the surface, thus explaining the peaks at 400.8 and 402.2 eV. Thus, the acid–base properties of the catalysts can influence the composition of the surface as determined by XPS. Figure 6 presents weight/weight percentages of nitrogen in the bulk and on the surface. Both measurements correlate quite well for AlPON precursors. However, fresh and reduced Pt–AlPON catalysts have a lower content of nitrogen on the surface than in the bulk. This may be due to the desorption of nitrogenous species from the surface of the catalysts during heating in the pretreatment vacuum chamber. As this effect is more important in the reduced Pt–AlPON series and is also observable even for similar contents of nitrogen, we can discard the effect of the different basicity due to the presence of nitrogen and we must relate this to the presence of platinum which favors the surface nitrogen loss.

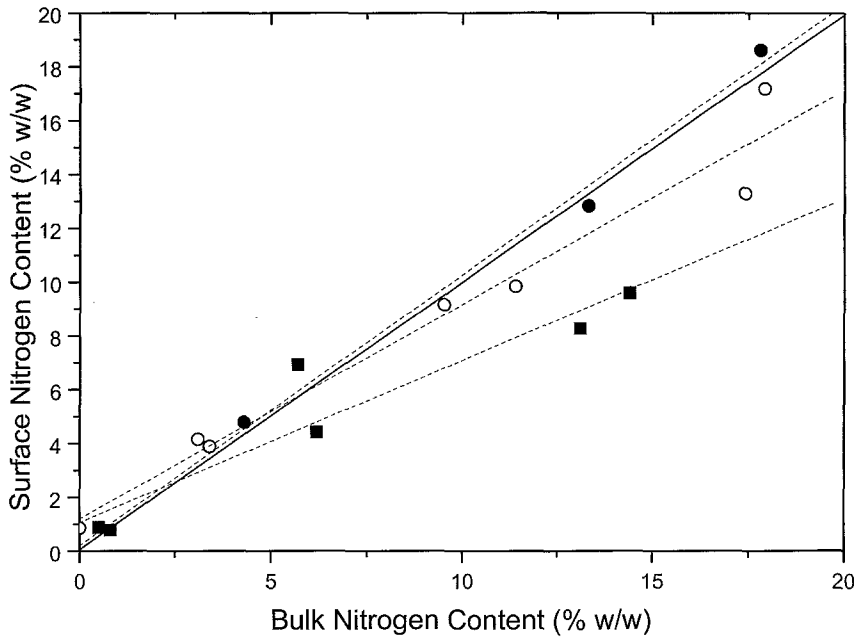

FIG. 6. Nitrogen content of the surface (from XPS measurements) versus nitrogen content of the bulk. (●) AlPON precursors, (○) fresh Pt–AlPON catalysts, and (■) reduced Pt–AlPON catalysts.

Catalytic Test

Table 3 shows initial isobutane conversions and isobutene selectivities obtained for the catalysts tested at the temperatures indicated. Isobutene selectivity is always around 90% indicating the low extension of the side reactions (isomerization, cracking, and hydrogenolysis). Thus, only traces of methane, ethane, ethylene, propane, propylene, *n*-butane, and *cis*- and *trans*-2-butene are observed for the most active catalysts at high temperatures. However, isobutane conversion varies considerably from one catalyst to another as well as with temperature. In general, initial isobutane conversion reaches a maximum at 520°C. The best yield of isobutene is about 56%, similar to that obtained with a commercial catalyst (2). At 430°C, no deactivation of the catalysts is detected after 14 h of reaction. However, at 480°C catalysts are deactivated rapidly. On the basis of carbon chemical analyses, this deactivation in Pt–AlGaPON catalysts has been related to the deposition of coke on the surface of the catalysts (25). Figure 7 shows the isobutene yield per unit of surface, at the lowest (430°C) and the highest (550°C) temperatures tested, as a function of the surface nitrogen content of the solid. For each series of catalysts, the isobutene yield increases with the increasing nitrogen content to a more or less constant value for surface nitrogen contents higher than 4–6 wt%. Furthermore, the series synthesized from $Pt(NH_3)_4(NO_3)_2$ is more active than that synthesized from $Pt(acac)_2$.

DISCUSSION

All the characterization techniques used in this study (XPS, DRIFTS, and SEM) do not differentiate between the

TABLE 3

Initial Isobutane Conversions (*C*) and Isobutene Selectivities (*S*) Obtained in the Catalytic Test

	430°C		480°C		520°C		550°C	
Sample	*C* (%)	*S* (%)	*C* (%)	*S* (%)	*C* (%)	*S* (%)	*C* (%)	*S* (%)
Pt–AlPO-a-R	8.71	92.21	8.46	89.44	8.75	84.69	6.93	85.08
Pt–AlPON4.3-a-R	0.71	100	1.28	100	1.66	100	1.74	100
Pt–AlPON4.3-n-R	0.84	100	1.85	100	1.79	100	1.55	100
Pt–AlPON13.3-a-R	18.67	73.65	50.71	85.30	66.28	82.79	67.61	83.23
Pt–AlPON13.3-n-R	19.75	92.94	23.65	91.74	45.63	91.74	42.93	91.95
Pt–AlPON17.8-a-R	11.60	98.76	29.10	95.62	31.09	94.46	24.64	94.88
Pt–AlPON17.8-n-R	18.60	94.38	42.84	90.39	49.40	90.47	42.29	91.61

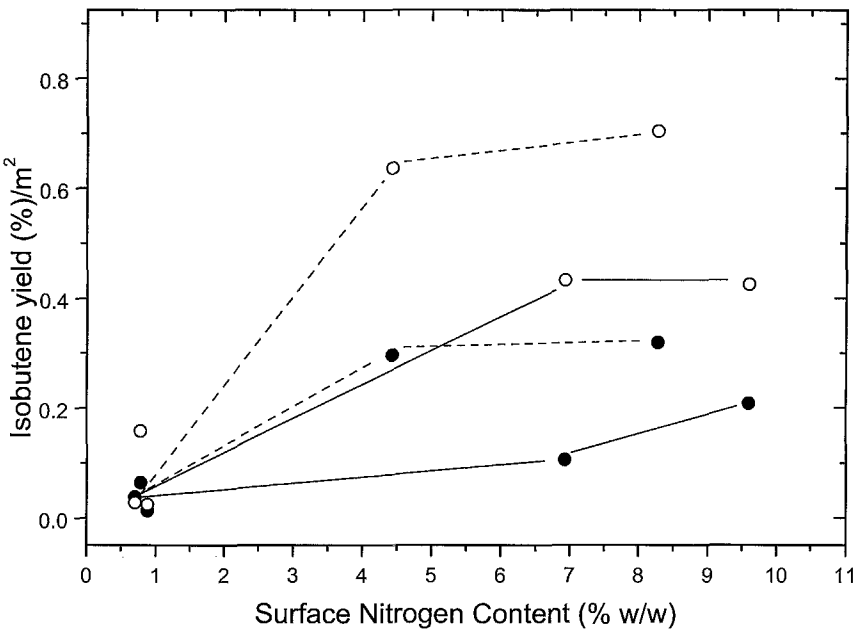

FIG. 7. Activity (isobutene yield per square meter) of Pt–AlPON catalysts as a function of the nitrogen content of the surface. (●) 430°C, (○) 550°C. Solid lines, catalysts from $Pt(acac)_2$; dashed lines, catalysts from $Pt(NH_3)_4(NO_3)_2$.

two series of Pt–AlPON catalysts. The differences among the solids arise only from the total nitrogen content and the concentration of the different nitrogen species, suggesting that the structure of the precursor is not modified during the impregnation and reduction steps.

The nature of the platinum precursor and the synthesis conditions influence both the final nitrogen content and the specific surface of the solids and has little effect on the dispersion of platinum. Thus, catalysts synthesized from $Pt(NH_3)_4(NO_3)_2$ always have a lower content of nitrogen and a smaller specific surface area than those synthesized from $Pt(acac)_2$, probably due to the water which hydrolyzes the solid surface. The presence of NO_3^- ions during synthesis can also contribute to the greater loss of nitrogen that is observed in catalysts derived from $Pt(NH_3)_4(NO_3)_2$; these anions can react with adsorbed ammonia species to give molecular nitrogen (26).

The nitrogen contents of the bulk and the surface of the AlPON precursors are similar (Fig. 6). However, for the Pt–AlPON catalysts, with high contents of nitrogen, the nitrogen content of the surface, as deduced from XPS, is always lower than the total content obtained by titration. These differences can be explained by the removal of nitrogenous species from the surface, mainly NH_4^+, as a result of the pretreatment in the XPS chamber (120°C, 10^{-6} Torr). As explained in the Results section, the acidity of the catalyst surface at low nitrogen contents is high; these species are strongly attached to the surface and remain there, even after pretreatment. In this case, the nitrogen contents of the surface and the bulk of AlPON precursors and Pt–AlPON catalysts are the same. However, at high nitrogen contents, the acidity of the surface is lower, and these species will probably be removed. In this situation, while the number of surface nitrogenous species removed from AlPON supports during pretreatment is within the measure error, it is too low to be detected in the Pt–AlPON solids. This suggests that the presence of platinum on the surface favors the loss of surface nitrogenous species during pretreatment. This effect is clearer in the reduced catalysts, indicating a stronger effect of the metallic state of the platinum atoms. On the other hand, no differences were found between the two series of catalysts.

When the nitrogen content of the solid increases, it becomes more basic, as can be deduced from the decrease in the binding energy of Al, P, O, and N atoms. However, at low nitrogen contents, surface nitrogenous species (–NH– and $-NH_2$ at high temperatures, and NH_4^+ at low temperatures) only are detected by DRIFTS. The surface concentration of these species increases with higher nitrogen contents until the entire surface is covered (about 6% w/w) (Fig. 2). At higher nitrogen contents, bulk nitridation begins. The composition of the surface, deduced from XPS, shows that as the nitrogen content of the surface increases, the numbers of surface ions (–NH– and $-NH_2$) and nitride ions increase (Fig. 5). A change in the slope (or a plateau) of the surface N^{3-}/NH_x ratio as a function of the total nitrogen content of the surface is observed when the nitrogen content reaches ≅11% (Fig. 8). This suggests a change in the structure of the surface of the catalysts. Thus, the incorporation of nitrogen into metallophosphates has been reported to

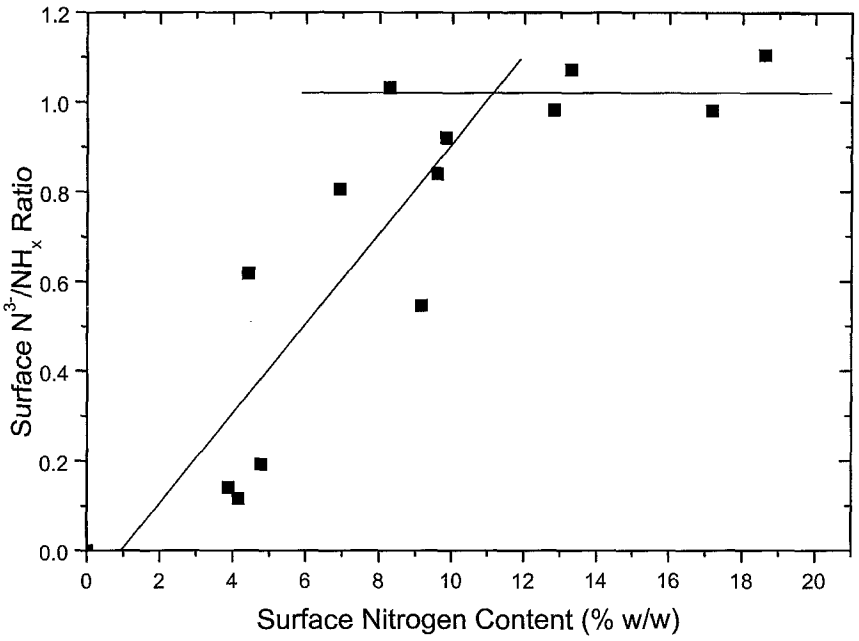

FIG. 8. Surface $N^{3-}/-NH_x$ ($x = 1, 2$) ratio as a function of the total nitrogen content of the surface of the solids (determined by XPS).

produce $[PO_3N]$ and $[PO_2N_2]$ polyhedra (27); it has been suggested that $[AlPO_4]$, $[AlPO_3N]$, and $[AlPO_2N_2]$ polyhedra form the bulk structure of AlPON solids, their proportion changing with the nitrogen/oxygen substitution ratio (17). A bulk structure consisting only of $[AlPO_3N]$ units gives an 11.6% (w/w) nitrogen content in the solid, very close to the experimental value observed from which the surface nitride-to-NH_x ratio changes. If only $[AlPO_2N_2]$ units were present, then the nitrogen content would be 23.5% (w/w). The maximum nitrogen content reported for aluminophosphate oxynitrides is 27.5% (w/w), which corresponds to the nitrogen content of $[AlPO_2N_2]$ (6). This change in structure could induce a change in the surface nitride-to-NH_x ($x = 1, 2$) species ratio. This change in the structure of the surface may be related to the bulk nitridation, as deduced from DRIFTS. The differences in the nitrogen content at which the change is observed arise from the different surface sensitivity of both techniques.

The activity of the catalysts seems to be related to the acid–base character of the catalysts, because the yield of isobutene per surface unit is a function of the nitrogen content (Fig. 8), and this parameter determines the sample basicity. The surface nitride-to-NH_x ratio is also related to the nitrogen content of the surface of the solid (Fig. 8) as well as to the activity. The plateau which activity reaches at high nitrogen contents is related to the change in the surface structure of the catalysts, as deduced from the plateau observed in Fig. 8.

Thereafter, the activity of the Pt–AlPON catalysts in the dehydrogenation of isobutane to isobutene seems to depend on the acid–base properties and on the structure of the solid. An increment in the nitrogen content of the solid makes it more basic, which has a positive effect on the activity. However, the ratio between the $[AlPO_4]$, $[AlPO_3N]$, and $[AlPO_2N_2]$ polyhedra present on the surface of the catalyst can be influenced by the synthesis conditions. This effect of structure can explain the higher activity of the catalysts synthesized from $Pt(NH_3)_4(NO_3)_2$. The use of water in the synthesis, which favors surface hydrolysis and the loss of surface nitrogenous species, or the different precursor–surface interactions, can all lead to a surface $[AlPO_xN_y]$ polyhedra ratio different from that obtained when using $Pt(acac)_2$ as the platinum precursor. However, since acidic and basic sites coexist in all solids and all these sites are active to some degree, both sites are probably needed for the reaction. Thus, activation of the C–H bond can occur by abstraction of a proton on a basic site, the anionic intermediate being stabilized on an adjacent acidic site. The structure of the solid also affects the activity, since it produces a change in the surface N^{3-}/NH_x ratio. The activation of the C–H bond would be the limiting step of the reaction, thus explaining the increase in the activity with increasing basicity of the solid. In the final step, another proton abstraction is produced and the alkene is formed and released from the surface. The surface of the catalyst is regenerated by the formation of gaseous H_2. The role of metallic platinum would be to increase the rate of this acid–base reaction by providing a porthole for hydrogen. The greater dispersion of platinum observed in the catalysts synthesized from $Pt(NH_3)_4(NO_3)_2$ compared to those prepared from $Pt(acac)_2$ (Table 1) can also contribute to the high activity of these samples. However, the differences in

Pt dispersion are negligible. In the sample with a moderate dispersion (Pt–AlPON4.3-n-R, 29.3%), the nitrogen content is so low (0.5% w/w) that the basicity of the solid is too low to enable high activity.

The deactivation observed at high temperatures has been related to the formation of coke on the surface of the catalyst (25). However, it has been reported that Pt–AlPON catalysts lose nitrogen as gaseous ammonia at high temperatures (14); thus, a change in the structure of the catalyst and/or in the nitrogen content of the solids during the reaction cannot be ruled out. This would make the catalysts less basic and would contribute to a decrease in the detected activity.

CONCLUSIONS

Pt–AlPON catalysts, prepared by impregnation of $Pt(acac)_2$ and $Pt(NH_3)_4(NO_3)_2$, are active catalysts for the dehydrogenation of isobutane to isobutene. The activity of these catalysts is a function of their basicity and the surface structure (ratio among the different $[AlPO_xN_y]$ polyhedra on the surface of the catalyst) of the solid. Since both basicity and surface structure are functions of the nitrogen content, special attention must be paid to the control of this parameter.

ACKNOWLEDGMENTS

M.A.C. thanks the European Union for a Training and Mobility of Researchers (TMR) Postdoctoral Grant (contract number ERBFMBI CT961182). The authors acknowledge the financial support of the FNRS and "Région Wallonne", Belgium.

REFERENCES

1. Takita, Y., Sano, K., Kurosaki, K., Kawata, N., Nishiguchi, H., Ito, M., and Ishihara, T., *Appl. Catal. A* **167**, 49 (1998).
2. Weckhuysen, B. M., and Schoonheydt, R. A., *Catal. Today* **51**, 223 (1999).
3. Guéguen, E., Kartheuser, B., Conanec, R., Marchand, R., Laurent, Y., and Grange, P., *in* "Proceedings of the DGMK Conference, Tagugngs bericht 9601" (J. Weitkamp and B. Lücke, Eds.), p. 235. DGMK Berichte, Berlin, 1996.
4. Delsarte, S., Guéguen, E., Massinon, A., Fripiat, N., Laurent, Y., and Grange, P., *in* "Proceedings of the DGMK Conference, Tagugngs bericht 9705" (W. Keim, B. Lücke, and J. Weitkamp, Eds.), p. 235. DGMK Berichte, Aachen, 1997.
5. Guéguen, E., Delsarte, S., Peltier, V., Conanec, R., Marchand, R., Laurent, Y., and Grange, P., *J. Eur. Ceram. Soc.* **17**, 2007 (1997).
6. Conanec, R., Marchand, R., and Laurent, Y., *High. Temp. Chem. Processes* **1**, 157 (1992).
7. Marchand, R., Conanec, R., Laurent, Y., Bastians, Ph., Grange, P., Gandia, L. M., Montes, M., Fernandez, J., and Odriozola, J. A., French Patent 94 01081, 1994.
8. Massinon, A., Odriozola, J. A., Bastians, Ph., Conanec, R., Marchand, R., Laurent, Y., and Grange, P., *Appl. Catal. A* **137**, 9 (1996).
9. Fripiat, N., Parvulescu, V., Parvulescu, V. I., and Grange, P., *Appl. Catal. A* **181**, 331 (1999).
10. Grange, P., Bastians, Ph., Conanec, R., Marchand, R., Laurent, Y., Gandia, L. M., Montes, M., Fernandez, J., and Odriozola, J. A., *Stud. Surf. Sci. Catal.* **91**, 381 (1995).
11. Courty, Ph., Ajot, H., Marcilly, Ch., and Delmon, B., *Powder Technol.* **7**, 21 (1973).
12. Delsarte, S., personal communication.
13. Centeno, M. A., Debois, M., and Grange, P., *J. Phys. Chem. B* **102**, 6835 (1998).
14. Centeno, M. A., and Grange, P., *J. Phys. Chem. B* **103**, 2431 (1999).
15. Benitez, J. J., Centeno, M. A., Odriozola, J. A., Conanec, R., Marchand, R., and Laurent, Y., *Catal. Lett.* **34**, 379 (1995).
16. Centeno, M. A., Delsarte, S., and Grange, P., *J. Phys. Chem. B* **103**, 7214 (1999).
17. Benitez, J. J., Diaz, A., Laurent, Y., and Odriozola, J. A., *Mater. Chem.* **8**, 687 (1998).
18. Benitez, J. J., Malet, P., Carrizosa, I., Odriozola, J. A., Conanec, R., Marchand, R., Laurent, Y., and Grange, P., *J. Eur. Ceram. Soc.* **17**, 1979 (1997).
19. Benitez, J. J., Diaz, A., Laurent, Y., Grange, P., and Odriozola, J. A., *Z. Phys. Chem.* **202**, 21 (1997).
20. Benitez, J. J., Centeno, M. A., Capitán, M. J., Odriozola, J. A., Viot, B., Verdier, P., and Laurent, Y., *J. Mater. Chem.* **5**, 1223 (1995).
21. Reidmeyer, M. R., Day, D. E., and Brow, R. K., *J. Non-Cryst. Solids* **103**, 35 (1988).
22. Grunze, M., *Surf. Sci.* **81**, 603 (1979).
23. Fripiat, N., Centeno, M. A., and Grange, P., *Chem. Mater.* **11**, 1434 (1999).
24. Wagner, C. D., Riggs, W. M., Davis, L. E., and Moulder, J. F., "Handbook of X-ray Photoelectron Spectroscopy." Perkin-Elmer Corp., Eden Prairie, MN, 1979.
25. Delsarte, S., Laurent Y., and Grange, P., *Mater. Sci. Forum* **51**, 325 (2000).
26. Dines, T. J., Rochester, C. H., and Ward, A. M., *J. Chem. Soc., Faraday Trans.* **87**, 1473 (1991).
27. Brow, R. K., Reidmeyer, M. R., and Day, D. E., *J. Non-Cryst. Solids* **99**, 178 (1988).